Treating disorder in introductory solid state physics

Dunkan Martínez,[a] Yuriko Baba,[b] and Francisco Domínguez-Adame[c]
GISC, Departamento de Física de Materiales, Universidad Complutense, Madrid E-28040, Spain

(Received 5 November 2022; accepted 2 June 2023)

Introductory textbooks in solid state physics present solvable models for illustrating the occurrence of allowed bands and forbidden gaps in the energy spectrum of Bloch electrons. However, the quantum mechanical description of electrons in non-periodic solids, such as amorphous materials, is beyond the scope of introductory courses because of its intrinsic complexity. The tight-binding approximation can account for such a scenario by letting the atomic levels vary at random from lattice site to site. We theoretically tackle the study of the average properties of the energy spectrum by introducing a transfer matrix method that allows us to obtain closed expressions for the so-called coherent potential. The coherent potential is energy-dependent and constant in space. It replaces the actual atomic random potential, thus generating a periodic effective medium with the same average properties as the non-periodic solid. We demonstrate that the average density of states can be calculated within this framework without relying on heavy mathematical machinery. Thus, our approach is suitable for introductory courses in solid state physics and materials science.

https://doi.org/10.1119/5.0133701

I. INTRODUCTION

The band theory of solids introduced by Felix Bloch paved the way to understand electron motion in crystals and the occurrence of allowed bands and forbidden gaps in the energy spectrum.[1] Shortly after Bloch's theory appeared, Ralph Kronig and William Penney considered a one-dimensional model of a periodic potential to describe the electron dynamics in an idealized crystal.[2] In its simplest form, the Kronig–Penney model corresponds to the Schrödinger equation for an electron moving in a periodic array of δ-function potentials. The resulting band structure is obtained exactly without requiring extensive computations, so it is often used in introductory textbooks to expose students to the main ideas behind the band theory of crystalline solids.[3–13]

However, disordered solids and amorphous materials are beyond the scope of introductory courses, because their constituent atoms are not arranged in a periodic manner, so Bloch's theory is not applicable. In his celebrated paper "Absence of diffusion in certain random lattices," Anderson tackled the problem of an electron in a three-dimensional random lattice.[14] Anderson established that the spatial fluctuations imposed on the wave function by the random potential lead to its localization when disorder exceeds a critical magnitude (see Ref. 15 for a comprehensive review). This phenomenon was named *Anderson localization* and led to his Nobel Prize in Physics in 1977 for fundamental theoretical investigations of the electronic structure of magnetic and disordered systems. Although a general overview of Anderson localization can be introduced to undergraduate students with the aid of simple reasoning and without sophisticated mathematical tools (see, e.g., Ref. 16 and references therein), the topic of electron states in noncrystalline solids is usually omitted from solid state physics courses because of its obvious complexity.

Anderson localization may occur when disorder enters via a random spatial distribution of elastic scattering sites.[15] The tight-binding approximation can account for such a scenario by assuming that the atomic levels vary randomly from site to site of the atomic lattice (see Ref. 16 for a brief introduction to the tight-binding approximation in the context of Anderson localization). Material systems where this model applies include metal alloys, such as CuNi and AgPd, and molecular systems. The scattering approach is the usual starting point for studying the average properties of the energy spectrum. In general, though, the configurationally averaged spectral properties cannot be calculated exactly and various approximations with different degrees of sophistication are employed. Among them, the *coherent potential approximation* (CPA) stands out because it interpolates properly between weak and strong scattering limits.[17] While several advanced textbooks in solid state physics provide thorough discussion of the CPA,[11,18,19] introductory textbooks addressing this approach are scarce[20] because advanced knowledge of a scattering theory is needed.[17]

In this paper, we bridge the gap between introductory and advanced textbooks by considering a one-dimensional (1D) model of a random binary alloy within the tight-binding approach. Disorder in 1D systems has its own peculiarities not shared by 3D systems. For instance, in 1D any amount of disorder results in the spatial localization of electrons, although the spatial extent of the wave function can be larger than the system size for weak disorder. This behavior is rather independent of the model of disorder (compositional or positional) and the distribution function of the random variables of the model (binary, uniform, Gaussian). So, in spite of the high impact of disorder, 1D systems are easier to study than their 3D counterparts.

In the CPA, the average electron properties of the disordered (non-periodic) solid are tackled by replacing the actual atomic random potential by one that is energy-dependent and the same at all lattice sites, usually referred to as the *coherent potential* in the literature.[17] The resulting effective medium is periodic with the same average properties as the non-periodic solid. In our approach, the coherent potential is obtained in a self-consistent way by means of the well-known transfer matrix method (TMM).[21,22] We demonstrate that the average density of states can be calculated without relying on advanced mathematical tools. Remarkably, the coherent potential obtained in this way turns out to be the same as the standard CPA result obtained by means of more

complicated mathematical tools (Green's functions method).[17] Therefore, our approach could be of interest to solid state physics instructors and students as it provides them with all necessary tools to understand advanced textbooks[17–19] and articles[23–25] dealing with the electronic structure of disordered materials.

II. ELECTRON STATES IN A 1D SOLID

Our starting point is the Schrödinger equation for a tightly bound electron in a 1D solid, assuming that only a single atomic orbital is relevant for the problem at hand.[5] The amplitude ψ_n of the electron wave function at the nth atom of the lattice satisfies the equation of motion (see, e.g., Ref. 16 for further details)

$$(E-\varepsilon_n)\psi_n - J\psi_{n+1} - J\psi_{n-1} = 0. \tag{1}$$

Here, E is the electron energy, ε_n is the energy of the atomic orbital of the nth atom, and J is the hopping (or tunneling) energy, which will be taken positive without loss of generality. The last two terms of Eq. (1) are related to the overlap of the wave functions of adjacent atoms.

A. 1D periodic monoatomic solid

Equation (1) is exactly solvable when the atomic levels are independent of n ($\varepsilon_n \equiv \bar{\varepsilon}$), because the lattice is periodic and Bloch's theorem holds. The amplitude of the wave function is, therefore, expressed as $\psi_n = A\exp(ikan)$, where k is the wave number, A is a normalization constant, and a is the lattice parameter. Inserting the Bloch wave ansatz into the equation of motion (1), we obtain the dispersion relation,

$$E_0(k) = \bar{\varepsilon} + 2J\cos ka, \tag{2}$$

where the subscript 0 refers to the periodic lattice. Here, k lies within the first Brillouin zone, $-\pi/a < k \le \pi/a$. Ignoring for simplicity the double degeneracy of electron states due to spin, the corresponding density of states per unit length (DOS) is $\rho_0(E,\bar{\varepsilon}) = (1/L)\sum_k \delta(E - E_0(k))$, where $L = Na$ is the length of the 1D solid with N atoms. Converting the summation into an integration over the first Brillouin zone, the DOS inside the band is

$$\begin{aligned}\rho_0(E,\bar{\varepsilon}) &= \frac{1}{2\pi}\int_{-\pi/a}^{\pi/a}\delta(E-E_0(k))\,\mathrm{d}k \\ &= \frac{1}{\pi}\int_{-\pi/a}^{0}\delta(E-E_0(k))\,\mathrm{d}k,\end{aligned} \tag{3a}$$

where we used $E_0(k) = E_0(-k)$. After performing a change of variables, the DOS is

$$\begin{aligned}\rho_0(E,\bar{\varepsilon}) &= \frac{1}{\pi}\int_{\bar{\varepsilon}-2J}^{\bar{\varepsilon}+2J}\delta(E-E_0(k))\,\frac{\mathrm{d}k}{\mathrm{d}E_0(k)}\,\mathrm{d}E_0(k) \\ &= \frac{1}{\pi}\left|\frac{\mathrm{d}k}{\mathrm{d}E_0(k)}\right|_{E_0(k)=E}\end{aligned} \tag{3b}$$

and vanishes outside the band. The DOS is of paramount importance in solid state physics since it is directly related to some important phenomena such as electrical conductivity in scanning tunneling microscopy, potential screening by electrons in metals, and optical absorption in semiconductors. Finally, recalling the dispersion relation (2), we obtain the DOS in the 1D periodic solid

$$\rho_0(E,\bar{\varepsilon}) = \frac{1}{\pi a\sqrt{4J^2 - (E-\bar{\varepsilon})^2}} \tag{4}$$

within the energy band. Notice that the DOS is singular at the two band-edges ($E = \bar{\varepsilon}\pm 2J$) due to the 1D nature of the periodic lattice.

B. 1D periodic binary solid

We now consider a slightly more complicated situation when there are two different atoms per unit cell, with energy levels ε_A and ε_B. Since the periodicity of the lattice is preserved and Bloch's theorem still holds, Eq. (1) is exactly solvable. The energy dispersion of the 1D periodic binary solid is found to be

$$E_\pm(k) = \frac{\varepsilon_A+\varepsilon_B}{2} \pm \sqrt{\frac{(\varepsilon_A-\varepsilon_B)^2}{4} + 4J^2\cos^2(ka/2)}, \tag{5}$$

and, recalling Eq. (3), the associated DOS is

$$\rho_0(E,\varepsilon_A,\varepsilon_B) = \frac{(\Delta_{EA}+\Delta_{EB})/\pi a}{\sqrt{(4J^2-\Delta_{EA}\Delta_{EB})\Delta_{EA}\Delta_{EB}}}, \tag{6}$$

where $\Delta_{EA} = E-\varepsilon_A$, $\Delta_{EB} = E-\varepsilon_B$, and a remains the lattice parameter. The DOS vanishes outside the bands, namely, when the denominator becomes imaginary.

Figure 1 displays the DOS as a function of energy, expressed in units of J, according to Eq. (6) when $\varepsilon_A = 0.6\,\mathrm{J}$ and $\varepsilon_B = 0$. We observe the occurrence of a gap separating two allowed energy bands and the DOS divergence at the four band edges. The gap appears for any nonzero value of the difference $\varepsilon_A - \varepsilon_B$, i.e., when the solid is truly diatomic. The magnitude of the gap increases with increasing $|\varepsilon_A - \varepsilon_B|$.

C. 1D disordered binary alloy

In a disordered lattice, on-site energies ε_n are different at different atomic positions. In addition, we will focus on binary disorder and assume that ε_n can take on two values, ε_A and ε_B, at random with probability c and $1-c$, respectively. Hence, the probability distribution of this model of the 1D binary alloy is

$$\mathcal{P}(\varepsilon_n) = c\delta(\varepsilon_n-\varepsilon_A) + (1-c)\delta(\varepsilon_n-\varepsilon_B). \tag{7a}$$

The configuration average over the probability distribution of any arbitrary function $f(\varepsilon_n)$ of the random variables ε_n is simply given as

$$\begin{aligned}\langle f(\varepsilon_n)\rangle_{\mathrm{av}} &= \int f(\varepsilon_n)\mathcal{P}(\varepsilon_n)\,\mathrm{d}\varepsilon_n \\ &= cf(\varepsilon_A) + (1-c)f(\varepsilon_B).\end{aligned} \tag{7b}$$

It should be mentioned that other probability distributions, such as Gaussian and uniform, can be handled in a similar way but we focus on binary disorder for the sake of concreteness. Figure 2(a) shows a schematic view of the 1D binary

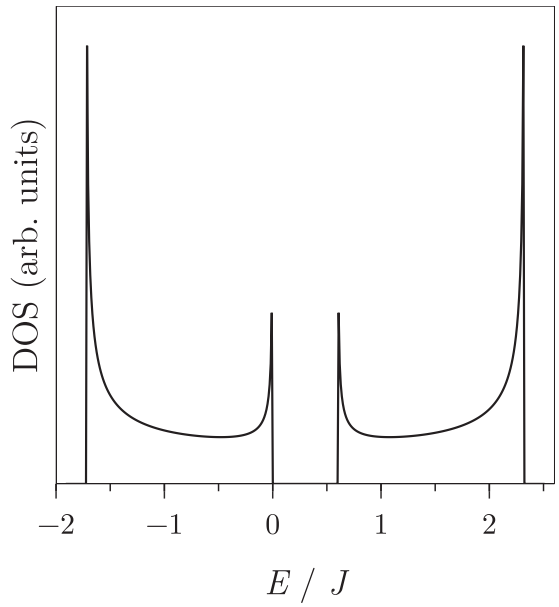

Fig. 1. Density of states (DOS) of a 1D periodic binary solid with on-site energies $\varepsilon_A = 0.6J$ and $\varepsilon_B = 0$ as a function of energy.

alloy, where the sequence of atomic levels with energy ε_A or ε_B is random.

For a given configuration of disorder, the equation of motion (1) can be solved by numerical diagonalization of a tridiagonal matrix, provided that the number of atoms N in the 1D binary alloy is not too large. Once the eigenenergies E_ν are known, the DOS is obtained as follows:

$$\rho(E) = \left\langle \frac{1}{L}\sum_{\nu} \delta(E - E_\nu) \right\rangle_{\text{av}}, \tag{8}$$

where ν in the sum runs over all eigenenergies. Here, as it is a disordered chain, there is a non-zero probability to find a region with a sufficiently long string of atoms of the same type. This means that the alloy DOS will extend over the same range as the energy bands of a periodic array of A atoms and a periodic array of B atoms.[26] This kind of *brute-force attack* was completely undoable in the early days of the electron theory of solids. It was then suggested that the electronic structure of a disordered binary alloy might be tackled by placing on each site of the atomic lattice an effective, or coherent, potential Σ [see Fig. 2(b)]. With this

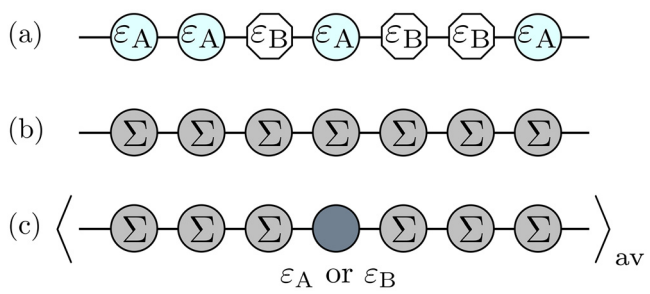

Fig. 2. (Color online) Pictorial representation of the calculation of the coherent potential. The disordered lattice is schematized in (a) and the effective medium is represented in (b). (c) The coherent potential Σ is determined from the condition that no further scattering happens on average when a single site of the effective medium is replaced by a site of the disordered lattice.

assumption, the translational symmetry is restored since the effective medium would be periodic, and the DOS would be given in Eq. (4) as $\rho_0(E, \Sigma)$. Therefore, the problem reduces to finding Σ such that $\rho_0(E, \Sigma) = \rho(E)$, where the latter is given in Eq. (8).

D. Virtual crystal approximation

For a first approximation of Σ, assume that the potential is given by the following average:

$$\Sigma_{\text{VCA}} \equiv \langle \varepsilon_n \rangle_{\text{av}} = c\varepsilon_A + (1 - c)\varepsilon_B. \tag{9}$$

This is known as the virtual crystal approximation (VCA) (see, e.g., Refs. 27 and 28). The VCA is a reasonably good description only if $\varepsilon_A \simeq \varepsilon_B$, the weak disorder regime, because the perturbed wave function is extended so the electron sees the average perturbation. More elaborate self-consistent approximations have a much wider range of validity, as we will show below.

E. Coherent potential approximation

Among other well-established approaches, the CPA is an excellent and accurate alternative to purely numerical calculations of the DOS.[29,30] The essential physical idea behind the CPA is to find the (yet unknown) *coherent potential* that defines the effective periodic medium, shown in Fig. 2(b), with the aid of some reasonable assumptions. This approximation is generally regarded as a single-site theory since electron scattering from clusters of impurities is neglected. Therefore, the CPA starts by removing one (and only one) atomic level Σ of the effective medium and in its place putting an actual atomic level ε_A or ε_B [see Fig. 2(c)]. The coherent potential Σ is determined by demanding that after the replacement by ε_A or ε_B, there is no further scattering on average. In other words, the CPA takes into account all scattering events with the *same* impurity and neglects scattering events with two or more impurities. The rigorous formulation of this condition requires advanced knowledge of a scattering theory beyond the introductory courses in solid state physics, as already discussed in the introduction. After complicated but otherwise straightforward calculations, the central equation of the CPA is found to be[17,28]

$$\left\langle \frac{\varepsilon_n - \Sigma}{1 + \mathrm{i}(\varepsilon_n - \Sigma)/\sqrt{4J^2 - (E - \Sigma)^2}} \right\rangle_{\text{av}} = 0, \tag{10}$$

where the configuration average is performed with the aid of Eq. (7b). This is an implicit equation for the coherent potential $\Sigma = \Sigma(E)$ that will be discussed in more detail later. In general, the coherent potential is complex and, according to the scattering theory, the real part represents an overall energy shift while the imaginary part is identified with the level broadening [see Eq. (14)].

We now present a simple methodology to arrive at the CPA equation, which preserves its underlying ideas with no need of the advanced scattering theory of quantum particles. Our approach relies on the well-known and easy-to-use transfer matrix method for 1D lattice problems.[21,22] We start by rewriting Eq. (1) in the matrix form

$$\begin{pmatrix} \psi_{n+1} \\ \psi_n \end{pmatrix} = P(\varepsilon_n) \begin{pmatrix} \psi_n \\ \psi_{n-1} \end{pmatrix}, \tag{11a}$$

where

$$P(\varepsilon_n) = \begin{pmatrix} (E-\varepsilon_n)/J & -1 \\ 1 & 0 \end{pmatrix} \tag{11b}$$

is known as the promotion matrix at a lattice position with on-site energy ε_n. The case of transmission when a single atomic level of the effective medium (say at site m) is replaced by either ε_A or ε_B, as depicted in Fig. 2(c), can be solved straightforwardly. We relate the amplitudes of the wave function at both sides of site m by iterating Eq. (11a)

$$\begin{pmatrix} \psi_{m+2} \\ \psi_{m+1} \end{pmatrix} = T(\varepsilon_m) \begin{pmatrix} \psi_{m-1} \\ \psi_{m-2} \end{pmatrix}, \tag{12a}$$

where $T(\varepsilon_m) \equiv P(\Sigma)P(\varepsilon_m)P(\Sigma)$ is the transfer matrix of the scattering region formed by sites $m-1$, m, and $m+1$. Notice that sites $m-1$ and $m+1$ are different from the other sites of the effective medium, in the sense that one of their two nearest-neighbors does not have an energy level Σ but rather ε_A or ε_B. Hence, sites $m-1$ and $m+1$ need to be regarded as part of the scattering region as well. After performing the matrix multiplication, the elements of the transfer matrix are found to be

$$\begin{aligned} T_{11}(\varepsilon_m) &= \frac{1}{J^3}(E-\Sigma)^2(E-\varepsilon_m) - \frac{2}{J}(E-\Sigma), \\ T_{12}(\varepsilon_m) &= 1 - \frac{1}{J^2}(E-\Sigma)(E-\varepsilon_m), \\ T_{21}(\varepsilon_m) &= -T_{12}\,\varepsilon_m, \\ T_{22}(\varepsilon_m) &= -\frac{1}{J}(E-\varepsilon_m). \end{aligned} \tag{12b}$$

The scattering region is connected to two semi-infinite lattices with on-site energy Σ. An electron incident from the left onto the scattering region can be reflected back to the left or transmitted to the right. Therefore, the amplitude of the total wave function is written as

$$\psi_n = \begin{cases} e^{ikna} + r_n e^{-ikna}, & n = m-1, m-2, \ldots \\ t_n e^{ikna}, & n = m+1, m+2, \ldots, \end{cases} \tag{13}$$

with r and t being the reflection and transmission amplitudes, respectively. Here, $k>0$ to ensure that the electron impinges from the left onto the scattering region. It must be borne in mind that the left and right semi-infinite lattices are periodic and, consequently, k is related to the electron energy in the effective medium as (see Sec. II A)

$$E_{\text{eff}}(k) = \Sigma + 2J\cos ka. \tag{14}$$

Inserting Eq. (13) in Eq. (12a) allows us to obtain the reflection amplitude as (see Appendix A)

$$r_m = \frac{T_{11}(\varepsilon_m) - T_{22}(\varepsilon_m) + T_{12}(\varepsilon_m)e^{-ika} - T_{21}(\varepsilon_m)e^{ika}}{T_{21}(\varepsilon_m) - T_{12}(\varepsilon_m) + T_{22}(\varepsilon_m)e^{ika} - T_{11}(\varepsilon_m)e^{-ika}} \times e^{ika(2m-3)}. \tag{15}$$

Finally, recalling Eq. (12b) and imposing the CPA condition regarding the absence of scattering on average, namely, $\langle r_n \rangle_{\text{av}} = 0$ where the average is given in Eq. (7b), we get

$$\left\langle \frac{\varepsilon_m - \Sigma}{1 + i(\varepsilon_m - \Sigma)/(2J\sin ka)} \right\rangle_{\text{av}} = 0, \tag{16}$$

when $0 < k \le \pi/a$. In conclusion, by virtue of Eq. (14), we find the same CPA equation (10) for the coherent potential using only the elementary scattering theory.

III. RESULTS

In order to simplify the expressions, we set the origin of energy at the energy level of B atoms, $\varepsilon_B = 0$. Performing the configurational average in Eq. (10) or Eq. (16) with the probability distribution (7a), and rearranging terms, the CPA equation can be cast in the following form:

$$\Sigma = \frac{c\varepsilon_A}{1 + i(\varepsilon_A - \Sigma)\Big/\sqrt{4J^2 - (E-\Sigma)^2}}. \tag{17}$$

The CPA equation (17) is an implicit equation for Σ which must be solved numerically for each energy of interest.[28] In general, the coherent potential Σ will be complex and, according to Eq. (14), there exists the possibility of obtaining complex energies $E(k)$ for real values of k. In cases like this, $\text{Im}(E_{\text{eff}}(k)) < 0$ gives the width associated with the state having energy $\text{Re}(E_{\text{eff}}(k))$.[19] Level broadening in disordered solids can also be understood from the perturbation theory: If the disordered potential is regarded as a perturbation, then it will mix Bloch states with different crystal wave number k. The variance of the perturbed levels turns out to be nonzero and can be identified with a broadening of the levels (see Ref. 16 for further details).

The solution of Eq. (17) is particularly simple in the limiting cases of strong and weak disorder. We start by considering these two limiting situations and compare the predicted DOS with the results obtained by direct diagonalization of the tridiagonal matrix Hamiltonian with rigid boundary conditions ($\psi_0 = \psi_{N+1} = 0$).

A. Strong disorder

Disorder is regarded as strong when $|\varepsilon_A|$ is large compared to the bandwidth $4J$. In this limit, we can make the approximation $\sqrt{4J^2 - (E-\Sigma)^2} \approx i(\Sigma - E)$ in Eq. (17), resulting in a real-valued coherent potential Σ. Inserting the obtained coherent potential in Eq. (14) leads to the following dispersion relation:

$$\begin{aligned} E^s_{\pm}(k) &= c\varepsilon_A + \gamma(k) \pm \sqrt{\gamma^2(k) + c(1-c)\varepsilon_A^2}, \\ \gamma(k) &\equiv J\cos ka + (1/2 - c)\varepsilon_A, \end{aligned} \tag{18}$$

where the superscript s indicates the strong disorder limit. Therefore, the energy spectrum splits into two bands in this limiting case. Once the dispersion relation is obtained, the DOS is calculated from Eq. (3) when $E_0(k)$ is replaced by $E^s_{\pm}(k)$. The solid line in Fig. 3 shows the obtained DOS for $c = 0.5$ and $\varepsilon_A = 6J$. The singularities of the DOS at the edges of the two bands are clearly observed in spite of the

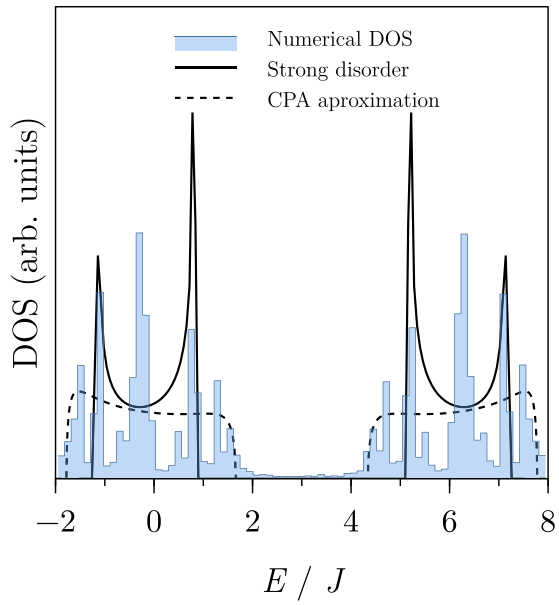

Fig. 3. (Color online) DOS in the strong disorder regime for $c = 0.5$ and $\varepsilon_A = 6J$. Solid line corresponds to the approximate dispersion relation (18). Filled curve displays the exact result after numerical diagonalization of the tridiagonal Hamiltonian for a 1D lattice with $N = 10\,000$, averaged over 500 realizations of disorder. Dashed line shows the CPA result after solving (17).

randomness of the system, a fact that it is deeply related to the absence of an imaginary part in the coherent potential (recall that the imaginary part gives the width of the energy level).

The shaded histogram in Fig. 3 displays the exact DOS obtained after numerical diagonalization of the tridiagonal Hamiltonian for a 1D lattice with $N = 10\,000$ sites (see Appendix B). The exact DOS is an average over 500 configurations with the same values of c and ε_A. Comparing the two plots, the approximate dispersion relation (18) is able to predict the splitting of the band, but the bandwidth is underestimated, leading to an overestimation of the bandgap. This inaccuracy is attributed to the approximations made to arrive at (18). To support this claim, the dashed line in Fig. 3 shows the CPA result after solving Eq. (17) exactly. Solution to this equation will be discussed later in this section. Clearly, the CPA result provides excellent values for the bandwidths and bandgap even in the strong disorder regime. However, it fails to take into account the sharp peaks observed in the numerical DOS that persist upon increasing the number of realizations of disorder. This failure is usually attributed to the single-site nature of the CPA [see Fig. 2(c)]. In other words, the CPA neglects the statistical fluctuations of the local environment of atoms in the alloy. Extensions of the CPA to deal with clusters of atoms have been developed, but they are beyond the scope of this work.[28]

B. Weak disorder

The weak disorder regime is established when $|\varepsilon_A|$ is smaller than the bandwidth $4J$. In this situation, Σ is expected not to differ much from $\Sigma_{VCA} = c\varepsilon_A$. Replacing Σ by $c\varepsilon_A$ in the right hand side of Eq. (17) leads to the following approximate dispersion relation:

$$E_{\text{eff}}(k) = 2J\cos ka + \frac{c\varepsilon_A}{1 + \mathrm{i}\,(1-c)\varepsilon_A \Big/ \sqrt{4J^2 - \left(E_{\text{eff}}(k) - c\varepsilon_A\right)^2}}, \tag{19}$$

which is easily solved to obtain $E_{\text{eff}}(k)$. It turns out to be complex, signaling the occurrence of a finite level width. Therefore, the δ-function in Eq. (3) needs to be replaced by a Lorentzian

$$\delta(E - E_{\text{eff}}(k)) \to \frac{1}{\pi}\frac{-\mathrm{Im}[E_{\text{eff}}(k)]}{\left\{E - \mathrm{Re}[E_{\text{eff}}(k)]\right\}^2 + \left\{\mathrm{Im}[E_{\text{eff}}(k)]\right\}^2}.$$

This replacement yields the proper limit in the absence of disorder, when the imaginary part of the coherent potential vanishes, according to the well-known result $\delta(x) = \lim_{\eta\to 0}(\eta/\pi)/(x^2 + \eta^2)$.

Figure 4 shows the DOS calculated using Eq. (19) for $c = 0.5$ and $\varepsilon_A = 0.6J$. This is compared to the exact DOS calculated by direct diagonalization of the tridiagonal Hamiltonian, shown by the filled curve. Although the approximate DOS is finite at the two band edges, it slightly overestimates the exact result. More accurate results are achieved by solving the exact CPA equation (17), shown by the dashed line in Fig. 4. Notice the excellent agreement between this and the numerical result in the weak disorder limit. It is worth mentioning that the singularities of the DOS at the band edges of the periodic solid observed in Fig. 1 are smeared out by disorder. This is a general trend in random alloys since substitutional disorder leads to the erosion of the van Hove singularities (see Ref. 24 for a discussion of this effect in disordered molecular crystals).

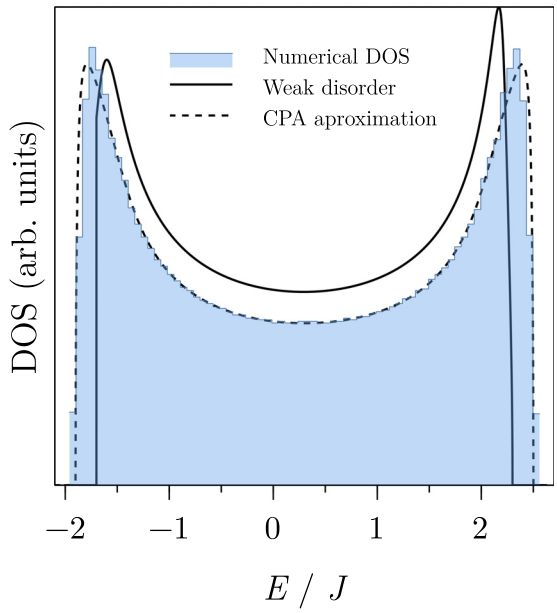

Fig. 4. (Color online) DOS in the weak disorder regime for $c = 0.5$ and $\varepsilon_A = 0.6J$. Solid line corresponds to the approximate dispersion relation (19). Filled curve displays the exact result after numerical diagonalization of the tridiagonal Hamiltonian for a 1D lattice with $N = 10\,000$, averaged over 500 realizations of disorder. Dashed line shows the CPA result after solving (17).

C. Solution of CPA equation

Equation (17) can be squared to render the following cubic equation for the coherent potential Σ:

$$
\begin{aligned}
&A_0\Sigma^3 + A_1\Sigma^2 + A_2\Sigma + A_3 = 0,\\
&A_0 \equiv 2E - 2(1-c)\varepsilon_A,\\
&A_1 \equiv 4J^2 - E^2 + (1-c^2)\varepsilon_A^2 - 4c\varepsilon_A E,\\
&A_2 \equiv 2c\varepsilon_A\left(c\varepsilon_A E - 4J^2 + E^2\right),\\
&A_3 \equiv c^2\varepsilon_A^2(4J^2 - E^2).
\end{aligned}
\tag{20}
$$

This cubic equation can be solved for $\Sigma(E)$ as a function of the two parameters c and ε_A. Once it is solved, the DOS is obtained as explained above.

Figure 5 shows the DOS for different magnitudes of disorder ε_A when $c = 0.5$. The single band observed in the weak disorder limit splits into two bands upon increasing the magnitude of disorder. The onset of band splitting occurs at $\varepsilon_A \sim 4\,J$. Gap opening by disorder has a strong impact on the optical properties of materials systems, as discussed by Onodera and Toyozawa in 1968, who showed that the behavior of the absorption coefficient is rather complex.[31] In addition, if the Fermi level moves through the gap that develops with increasing disorder, then a metal/insulator transition occurs.

Finally, Fig. 6 shows the DOS for different concentrations c when the magnitudes of disorder are $\varepsilon_A = 2J$. We observe that the single band limit is restored upon increasing c above 0.2 for this magnitude of disorder. This is consistent with what is described in Secs. II B and II C, since as c increases so does the probability of finding a sufficiently long chain of atoms with the same energy ε_A or ε_B.

IV. CONCLUSIONS

Electron motion in disordered solids has been an active field of research for the past 60 years. However, the absence of translational symmetry makes theoretical analysis highly complex, and there are few introductory-level treatments of important disorder-related phenomena such as localization and metal-insulator transitions. In particular, the CPA is usually derived using advanced mathematical tools such as Green's functions and is typically beyond the scope of undergraduate coursework in solid state physics. Our approach to the CPA, based on the transfer matrix method, arrives at the same results without the heavy mathematical overload. This makes the treatment of disordered phenomena accessible to undergraduate or early graduate students.

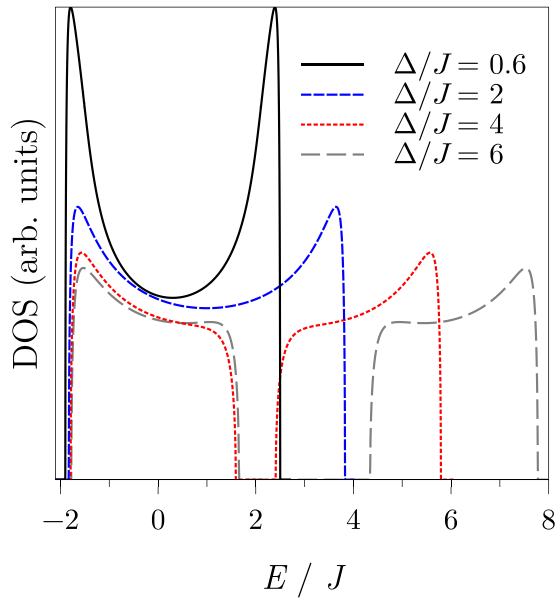

Fig. 5. (Color online) DOS for a 1D binary alloy as a function of the magnitude of disorder ε_A when $c = 0.5$.

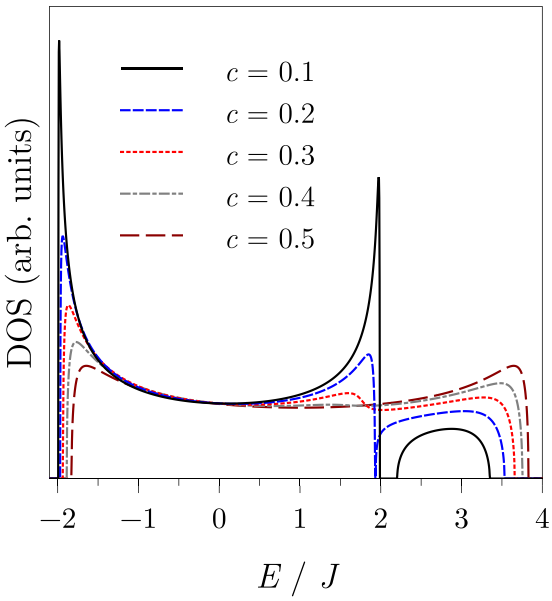

Fig. 6. (Color online) DOS for a 1D binary alloy as a function of the concentration c when $\varepsilon_A = 2J$.

ACKNOWLEDGMENTS

The authors thank A. Díaz-Fernández for helpful discussion. This work has been supported by Ministerio de Ciencia e Innovación (Grant No. PID2019–106820RB-C21). The authors also acknowledge the support from the "(MAD2D-CM)-UCM" project funded by Comunidad de Madrid, by the Recovery, Transformation and Resilience Plan, and by NextGenerationEU from the European Union.

AUTHOR DECLARATIONS

Conflict of Interest

The authors have no conflicts of interest to disclose.

APPENDIX A: CALCULATION OF THE REFLECTION COEFFICIENT

After inserting Eq. (13) into Eq. (12a) and dividing by $e^{ika(m-1)}$, one gets

$$
\begin{aligned}
te^{i3ka} &= M_1^-(\varepsilon_m) + re^{-2ika(m-1)}M_1^+(\varepsilon_m),\\
te^{i2ka} &= M_2^-(\varepsilon_m) + re^{-2ika(m-1)}M_2^+(\varepsilon_m),
\end{aligned}
\tag{A1}
$$

where $M_i^{\pm}(\varepsilon_m) = T_{i1}(\varepsilon_m) + T_{i2}(\varepsilon_m)e^{\pm ika}$. Dividing one equation by the other and solving for r yields

$$r_m = \frac{M_1^-(\varepsilon_m) - M_2^-(\varepsilon_m)e^{ika}}{M_2^+(\varepsilon_m)e^{ika} - M_1^+(\varepsilon_m)}\, e^{2ika(m-1)}, \tag{A2}$$

which can be easily converted into Eq. (15) by recalling the definition of $M_i^{\pm}(\varepsilon_m)$.

APPENDIX B: NUMERIC SIMULATION CODE

The code has been written using Python as the programming language. Therefore, we need to import the packages to be used

```
import numpy as np
from scipy.linalg import eigvalsh_tridiagonal
```

Then, we will define the diagonal of the Hamiltonian, which will be filled with randomly on-site energies following the probability distribution (7a). The system will have *N* sites, the on-site energies will be *eps_a* and *eps_b*, and the hopping will be *J*.

```
def r_hamiltonian(N, c, eps_a, eps_b, J):
  diag = []
  for i in range(N):
    rn = np.random.rand()
    if rn > c:
      diag.append(eps_b)
    else:
      diag.append(eps_a)
```

Once we have the diagonal elements defined, we will populate the off-diagonal matrix elements and then calculate the eigenvalues. They will be sorted in order to make the configurational average in the next step.

```
RE = np.sort(eigvalsh_tridiagonal(diag,
     J*np.ones(N-1)))
return RE
```

Now, we will take the average of *N_prom* realizations of disorder.

```
def Prom(N_prom, N, c, eps_a, eps_b, J):
  M = [r_hamiltonian(N, c, eps_a, eps_b, J)
  for i , in ↪range(N_prom)]
  eig = np.moveaxis(M,0,-1)
  E = np.mean(eig,1)
  return E
```

Finally, to find the numerical DOS from the disorder chain, we need to make an histogram with the averaged energies.

[a]Electronic mail: dunmar01@ucm.es, ORCID: 0000-0003-1106-9698.
[b]Electronic mail: yuribaba@ucm.es, ORCID: 0000-0003-0647-3477.
[c]Electronic mail: adame@ucm.es, ORCID: 0000-0002-5256-4196.

[1]F. Bloch, "Über die quantenmechanik der elektronen in kristallgittern," Z. Phys. **52**, 555–600 (1929).
[2]R. de L. Kronig and W. G. Penney, "Quantum mechanics of electrons in crystal lattices," Proc. R. Soc. London Ser. A **130**, 499–513 (1931).
[3]A. J. Dekker, *Solid State Physics* (Prentice-Hall, New Jersey, 1960).
[4]R. A. Smith, *Wave Mechanics of Crystalline Solids* (Chapman & Hall, London, 1969).
[5]N. W. Ashcroft and N. D. Mermin, *Solid State Physics* (Saunders College, Philadelphia, 1976).
[6]J. P. McKelvey, *Solid State and Semiconductor Physics* (Krieger Publishing Company, Florida, 1982).
[7]U. Mizutani, *Introduction to the Electron Theory of Metals* (Cambridge U. P., Cambridge, 2001).
[8]E. O'Reilly, *Quantum Theory of Solids* (Taylor & Francis, New York, 2002).
[9]L. Mihály and M. C. Martin, *Solid State Physics: Problems and Solutions* (John Wiley & Sons, New York, 2009).
[10]M. Razeghi, *Fundamentals of Solid State* (Springer, Berlin, 2009).
[11]E. N. Economou, *The Physics of Solids: Essentials and Beyond* (Springer, Berlin, 2010).
[12]G. Grosso and G. P. Parravicini, *Solid State Physics* (Elsevier Science, Amsterdam, 2013).
[13]J. Patterson and B. Bailey, *Solid-State Physics: Introduction to the Theory* (Springer, Berlin, 2016).
[14]P. W. Anderson, "Absence of diffusion in certain random lattices," Phys. Rev. **109**, 1492–1505 (1958).
[15]D. Vollhardt, "Localization effects in disordered systems," in *Advances in Solid State Physics*, edited by P. Grosse (Springer, Berlin, 1987), p. 63.
[16]F. Domínguez-Adame and V. A. Malyshev, "A brief introduction to Anderson localization," Am. J. Phys. **72**, 226–230 (2004).
[17]E. N. Economou, *Green's Functions in Quantum Physics* (Springer, Berlin, 2006).
[18]W. Jones and N. March, *Theoretical Solid State Physics: Non-Equilibrium and Disorder* (Dover Publications, New York, 1985).
[19]J. Callaway, *Quantum Theory of the Solid State* (Elsevier, Amsterdam, 2013).
[20]J. E. Hasbun and T. Datta, *Introductory Solid State Physics with MATLAB Applications* (CRC Press, Boca Raton, 2019).
[21]P. D. Kirkman and J. B. Pendry, "The statistics of one-dimensional resistances," J. Phys. C: Solid State Phys. **17**, 4327–4344 (1984).
[22]J. S. Walker and J. Gathright, "Exploring one-dimensional quantum mechanics with transfer matrices," Am. J. Phys. **62**, 408–422 (1994).
[23]B. Velický, "Theory of electronic transport in disordered binary alloys: Coherent-potential approximation," Phys. Rev. **184**, 614–627 (1969).
[24]J. Hoshen and J. Jortner, "Application of the coherent potential approximation to the excited electronic states of substitutionally disordered molecular crystals," J. Chem. Phys. **56**, 5550–5575 (1972).
[25]A. Maurel and P. A. Martin, "Propagation in one-dimensional crystals with positional and compositional disorder," Eur. Phys. J. B **86**, 486 (2013).
[26]P. Soven, "Band structure in disordered alloys and impurity semiconductors," Phys. Rev. **156**, 809–813 (1967).
[27]N. E. Cusack, *The Physics of Structurally Disordered Matter* (Adam Hilger, Bristol, 1988).
[28]A. Gonis, *Green Functions for Ordered and Disordered Systems* (North-Holland, Amsterdam, 1992).
[29]E. De Dycker and P. Phariseau, "Bandtailing in a disordered Kronig-Penney model," Physica **31**, 1337–1345 (1965).
[30]F. Le Vot, J. J. Meléndez, and S. B. Yuste, "Numerical matrix method for quantum periodic potentials," Am. J. Phys. **84**, 426–433 (2016).
[31]Y. Onodera and Y. Toyozawa, "Long wavelength optical phonons in mixed crystals," J. Phys. Soc. Jpn. **24**, 341–355 (1968).